ASTROBIOLOGY
Volume 6, Number 3, 2006

Special Paper

Oxidant Enhancement in Martian Dust Devils and Storms: Storm Electric Fields and Electron Dissociative Attachment

GREGORY T. DELORY,[1] WILLIAM M. FARRELL,[2] SUSHIL K. ATREYA,[3] NILTON O. RENNO,[3] AH-SAN WONG,[3] STEVEN A. CUMMER,[4] DAVIS D. SENTMAN,[5] JOHN R. MARSHALL,[6] SCOT C.R. RAFKIN,[7] and DAVID C. CATLING[8,9]

ABSTRACT

Laboratory studies, numerical simulations, and desert field tests indicate that aeolian dust transport can generate atmospheric electricity via contact electrification or "triboelectricity." In convective structures such as dust devils and dust storms, grain stratification leads to macroscopic charge separations and gives rise to an overall electric dipole moment in the aeolian feature, similar in nature to the dipolar electric field generated in terrestrial thunderstorms. Previous numerical simulations indicate that these storm electric fields on Mars can approach the ambient breakdown field strength of ~25 kV/m. In terrestrial dust phenomena, potentials ranging from ~20 to 160 kV/m have been directly measured. The large electrostatic fields predicted in martian dust devils and storms can energize electrons in the low pressure martian atmosphere to values exceeding the electron dissociative attachment energy of both CO_2 and H_2O, which results in the formation of the new chemical products CO/O^- and OH/H^-, respectively. Using a collisional plasma physics model, we present calculations of the CO/O^- and OH/H^- reaction and production rates. We demonstrate that these rates vary geometrically with the ambient electric field, with substantial production of dissociative products when fields approach the breakdown value of ~25 kV/m. The dissociation of H_2O into OH/H^- provides a key ingredient for the generation of oxidants; thus electrically charged dust may significantly impact the habitability of Mars. Key Words: Mars—Dust storm—Dust devil—Electric field—Oxidant—Habitability. Astrobiology 6, 451–462.

[1]Space Sciences Laboratory, University of California, Berkeley, Berkeley, California.
[2]Laboratory for Extraterrestrial Physics, NASA Goddard Space Flight Center, Greenbelt, Maryland.
[3]Department of Atmospheric, Oceanic, and Space Sciences, University of Michigan, Ann Arbor, Michigan.
[4]Department of Electrical and Computer Engineering, Duke University, Durham, North Carolina.
[5]Geophysical Institute, University of Alaska, Fairbanks, Alaska.
[6]SETI Institute, Mountain View, California.
[7]Southwest Research Institute, Boulder, Colorado.
[8]Department of Atmospheric Sciences/Astrobiology Program, University of Washington, Seattle, Washington.
[9]Department of Earth Sciences, University of Bristol, Bristol, United Kingdom.

INTRODUCTION

A CENTRAL QUESTION relevant to the habitability of Mars relates to the origin and presence of oxidants in the atmosphere and soil (Klein, 1998), which may have sterilized the surface and hence led to the failure of the Viking life sciences experiments to detect organics (Oyama *et al*., 1977). Photochemical processes have been invoked to explain the presence of oxidants on Mars, with hydrogen peroxide (H_2O_2) the most likely product (Krasnopolsky, 1993, 1995; Atreya and Gu, 1994; Nair *et al*., 1994; Clancy and Nair, 1996). While the recent discovery of H_2O_2 at 20–40 parts per billion volume on Mars (Encrenaz *et al*., 2004) is consistent with production by photochemical processes in the atmosphere, the soil reactivity implied by the Viking results indicate levels ranging from at least 1 part per million (Zent and McKay, 1994) up to ~250 parts per million (Mancinelli, 1989). The short lifetime of H_2O_2 in the atmosphere relative to its rate of diffusion into the soil makes the production of the inferred levels of oxidants difficult to explain from photochemical processes alone, and thus additional sources should be explored. Mills (1977) was one of the first to consider an alternative production mechanism when he suggested that the electrification in dust storms may be an added physiochemical energy source that has the ability to create a number of new species, including the oxidant H_2O_2. Oyama and Berdahl (1979) described the possible creation of an oxygen plasma from dust electrification on Mars, while Ballou *et al*. (1978) showed that oxygen plasmas can create oxidants when exposed to basalts.

Here we investigate the implications of the ubiquitous presence of strong electric fields on Mars for atmospheric chemical processes relevant to oxidant production, which result from the ionization and dissociation of H_2O by energized electrons in the martian atmosphere. Large electrostatic fields created by dust devils and storms or other aeolian processes can lead to the creation and energization of electrons as an ambient core population is accelerated and the ionization of CO_2 occurs. Using a detailed numerically based plasma physics model, we calculate the electron energy distribution for electric fields ranging from small values (~5 kV/m) to levels near the breakdown potential (~25 kV/m) that would be present in a given dust storm event. We then study the impact of this process on the local atmospheric chemistry with an emphasis on products relevant to subsequent oxidant formation. Under these conditions we find that the dissociation of H_2O *via* electron collisions produces negative ions at rates that vary strongly with the applied electric field and become greater than photochemical rates by several orders of magnitude. The generation of OH/H^- will lead to the subsequent production of H_2O_2 at rates greater than photochemical processes (Atreya *et al*., 2006). This process would be common in the lower atmosphere down to the surface and predominant when high atmospheric dust loads attenuate photochemical processes. This ubiquitous, rapid source of oxidants would provide strong support for the interpretation of the Viking results as indicative of a chemically reactive, oxidant-rich soil. This mechanism also has implications for the lifetime and spatial distribution of methane, recently measured in the atmosphere of Mars (Formisano *et al*., 2004; Krasnopolsky *et al*., 2004; Mumma *et al*., 2004).

THE ELECTRIC DUST STORM

The dynamic martian atmosphere is characterized by ubiquitous aeolian activity, with significant dust lofting and transport occurring over a wide dynamic range of spatial and temporal scales. Global dust storms can envelope a significant fraction of the planet, and appear to be seasonally dependent in that a large number of these storms occur between southern spring and summer, around perihelion (Martin and Zurek, 1993). Over 780 local to regional (~10^2–10^6 km^2) dust storms during the 1999 storm season have been cataloged by Cantor *et al*. (2001), who studied the geographic and seasonal dependencies of these events. The most common dust activity on Mars occurs at the smallest scale; warm-cored, convective vortices such as dust devils are likely present to varying extents during most seasons (Newman *et al*., 2002; Fisher *et al*., 2005). Dust devils with diameters between 100 m and 1 km, and heights of up to 5–10 km, are frequently observed on Mars (Thomas and Gierasch, 1985; Fisher *et al*., 2005). Based on their Mars Global Surveyor-observed tracks, Mars' dust devils are found at nearly all locations on the planet, and because of their dynamic nature, they are continuously removing dust from the surface and maintaining the bulk atmospheric dust opacity during non-

a

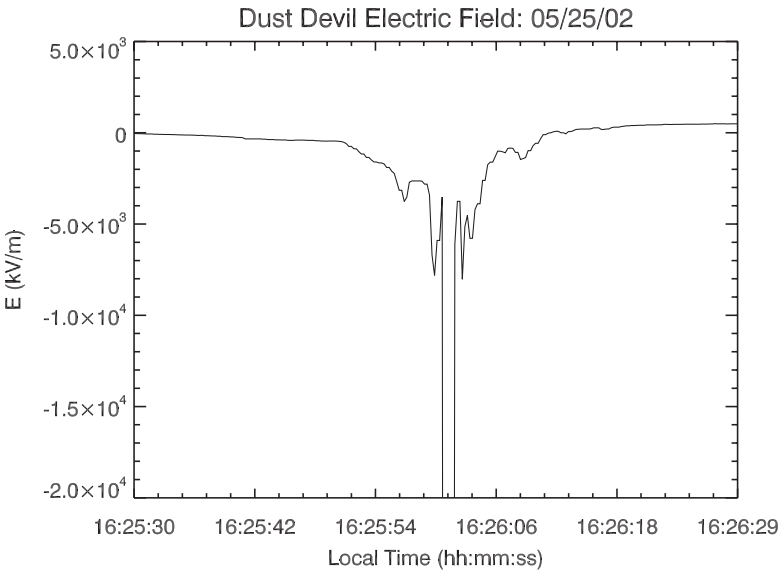

FIG. 1. **a:** Terrestrial electric field measurements of dust devils such as this event near Eloy, AZ. Maximum electric fields occur near the core of the events, in many cases saturating the instrument with readings below −20 kV/m. **b:** Models for both macro- and microelectrification in a dust devil. Larger dust storm electrification is envisioned to occur in a similar manner.

b Martian Dust Devil

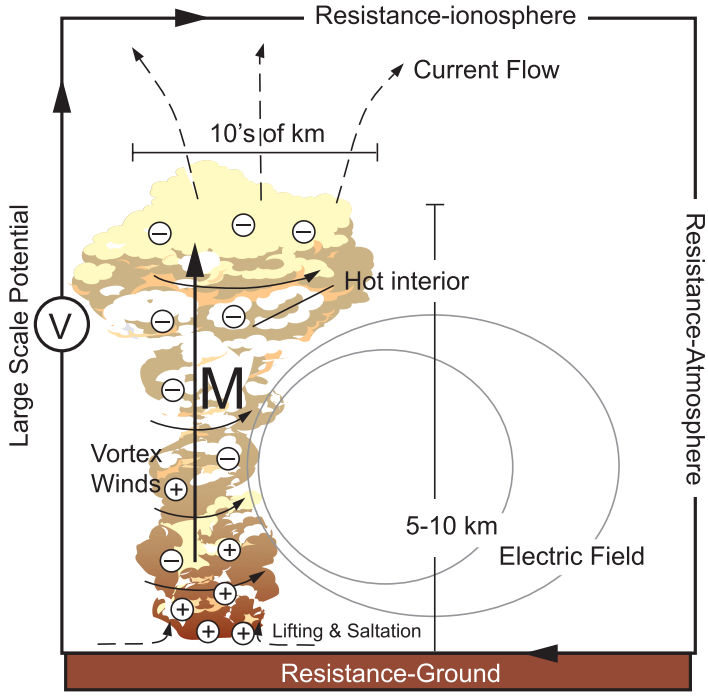

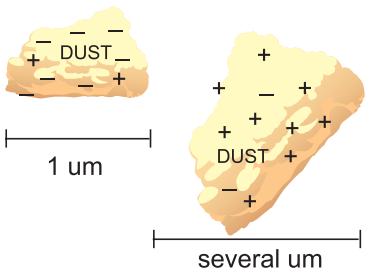

Triboelectric charging: friction between dust grains or dust and the surface leads to the separation of charge.

Stratification of dust grains leads to the macroscopic separation of charge (left)

storm seasons (Ryan and Lucich, 1983; Smith and Lemmon, 1999; Ferri *et al.*, 2003).

Experimental and theoretical investigations of frictional charging mechanisms in both small- and large-scale meteorological phenomena suggest that Mars very likely possesses an electrically active atmosphere as a result of dust-lifting processes of all scales, including dust devils and dust storms. Naturally occurring dust activity is nearly always associated with significant electrification *via* the process of triboelectricity—the frictional charging of dust grains in contact with one another or the surface as they are transported by wind or convective circulations. In terrestrial systems, early studies clearly demonstrated the presence of electric fields in the kilovolt/meter range within about 100 m of dust devils (Freier, 1960; Crozier, 1964, 1970). More recently, electric fields ranging from ~3 kV/m to greater than 20 kV/m have been measured within dust devils, as shown in Fig. 1a (Farrell *et al.*, 2003, 2004; Renno *et al.*, 2004). Surface processes can also generate significant electrification. In saltating sand, in which impacts from sand particles on approximately centimeter-scale ballistic trajectories generate lofted dust, fields in excess of 160 kV/m have been measured within the first few centimeters of the surface (Schmidt *et al.*, 1998). The largest terrestrial dust events, volcanic plumes, can generate lightning, and thus serve as a demonstration that electrified dust can indeed reach breakdown potentials (Anderson, 1965). Contact electrification can lead to differential charging of dust grains *via* a variety of mechanisms; in events with grains of similar composition, smaller particles typically obtain a net negative charge, while larger particles become positive (Ette, 1971; Melnik and Parrot, 1998; Farrell *et al.*, 2003; Renno *et al.*, 2003). Thus a large-scale electric dipole moment can be generated by nearly any process with a vertical lifting component, as the smaller, negatively charged grains are transported to higher altitudes than the heavier, positively charged grains. In dust devils and dust storms, the vertical stratification of grains based on size and mass will create a stratification of charge, which creates an electric dipole moment with a spatial scale on the order of the storm size (Fig. 1b). Based on the results of terrestrial experiments and their implications for the presence of electrification processes on Mars, Melnick and Parrot (1998) used a particle-in-cell numerical model to show that electric fields up to the breakdown potential of 25 kV/m can easily occur near the martian surface.

DUST STORM-DRIVEN ELECTRON ENERGIZATION

The martian troposphere may be considered as a tenuous electron plasma due to the presence of a high-density neutral background dominated by electron-neutral collisional processes. Based on the penetration of ionizing radiation from cosmic rays and radioactive elements in the martian crust, a representative core population electron density near the surface is $n_e \sim 5 \times 10^6/\mathrm{m}^3$ (Whitten *et al.*, 1971). These electrons interact with the ambient CO_2 *via* a multitude of collisional processes with cross sections that vary strongly with energy. At low energies (<1 eV), elastic scattering and momentum transfer determine the electron drift velocities through the medium. In the range of 1–10 eV, CO_2 possesses large cross sections for vibrational and electronic excitation through electron collisions.

An important process in this energy range is dissociative attachment, in which an electron attaches to a CO_2 molecule, which then rapidly dissociates into a negative ion and a neutral molecule. Electron attachment processes are an important part of the chemistry of the terrestrial atmosphere, where they are the dominant means by which negative ions are produced from O_2 (Viggiano and Arnold, 1995). In dissociative attachment, the following reaction occurs:

$$e + AB \rightarrow A^- + B \quad (1)$$

A second process, associative electron attachment, involves a third body:

$$e + AB + M \rightarrow AB^- + M \quad (2)$$

In the lower terrestrial atmosphere, the three-body process dominates. However, at higher altitudes and under an appreciable electric field, electron dissociative attachment is the dominate mechanism for free electron removal and negative ion formation, particularly near discharge events in the vicinity of thunderstorm activity.

The behavior of tenuous electron plasmas in the presence of a neutral CO_2 background was investigated numerically by Nighan (1970), who considered a range of electron–CO_2 collisional

processes in the presence of an electric field for parameters relevant to Mars. In this approach the electron distribution is described by the Boltzmann equation:

$$-\frac{e\vec{E}}{m_e}\cdot\nabla_v f(\vec{v}) = \left[\frac{\partial f(\vec{v})}{\partial t}\right]_c \qquad (3)$$

where e is the electron charge, m_e is the electron mass, $\vec{E}$ is the applied electric field, and $f(\vec{v})$ is the electron distribution as a function of the three-dimensional velocity vector $\vec{v}$. The subscript c on the right-hand side of Eq. 3 denotes effects due to electron collisions and is a sum over all relevant collisional cross sections describing electron–CO_2 interactions, including momentum transfer, vibrational and electronic excitations, dissociative attachment, and impact ionization. Figure 2 shows graphically some of these interactions, *i.e.*, electron impact ionization and dissociation of both CO_2 and H_2O, including the relevant electron energies. In Eq. 3, the acceleration

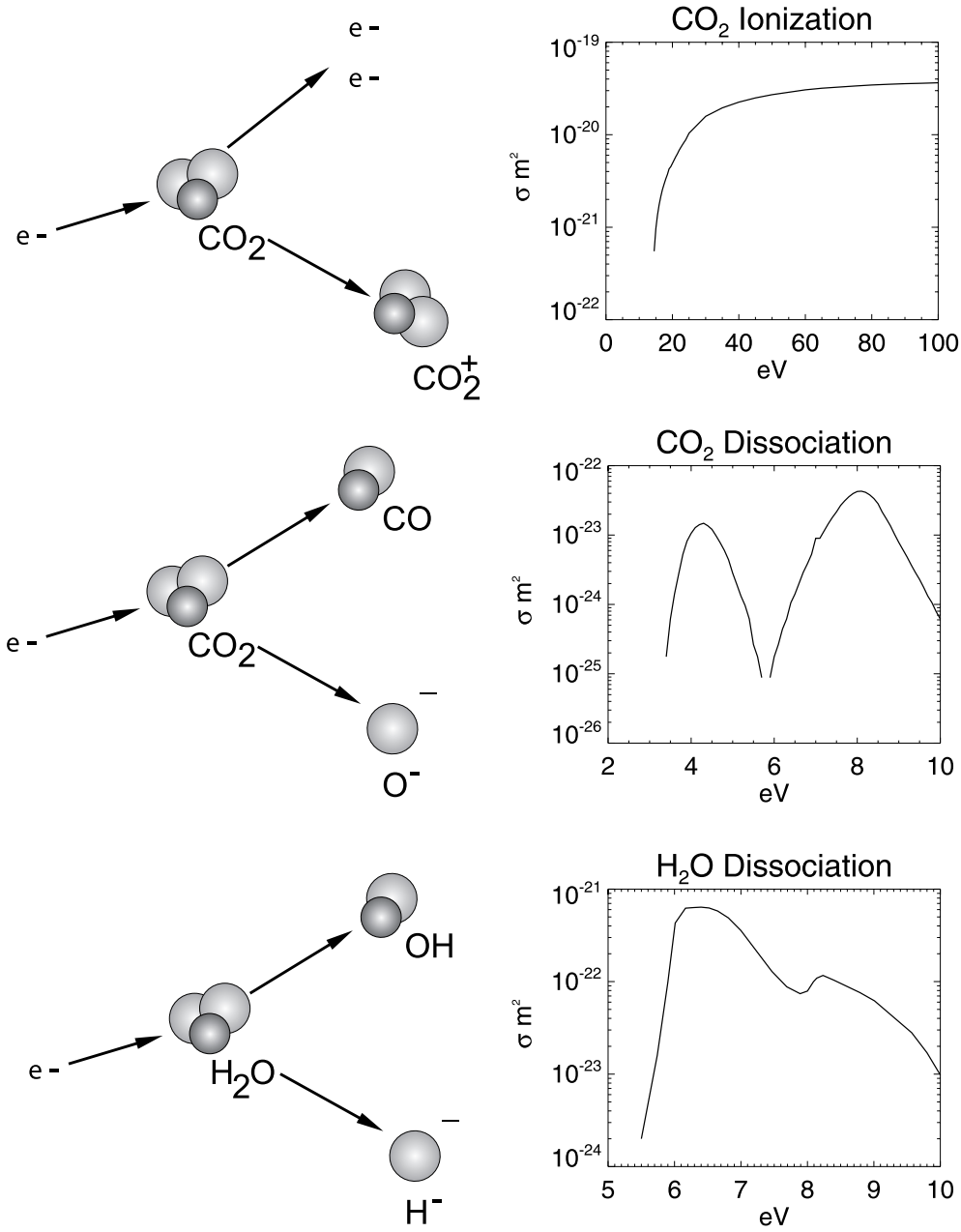

FIG. 2. Electron–CO_2 and –H_2O impact processes. Cross-section data shown for CO_2 ionization and dissociation were compiled by Itikawa (2002); H_2O dissociation cross-section data were provided by Itikawa and Mason (2005).

of the electrons via the electric force is offset by energy-depleting interactions with the CO_2 molecule, which occur on spatial scales of the mean free path; the combination of these effects can create a statistical electron energy distribution that varies substantially from a Maxwellian distribution. The average electron energy increases with electric field strength, which results in the development of a high-energy tail in the electron energy distribution.

Numerical solutions to Eq. 3 can be found based on the Pitchford, O'Neil, and Rumble (POR) technique (Pitchford *et al*., 1981). For the electron–CO_2 interactions on the right-hand side of Eq. 3, we consider the vibrational, excitational, attachment, and ionization processes shown in Table 1. The values of electric field E we use range from ~5 kV/m to near the theoretical breakdown potential of ~25 kV/m for Mars. Solutions to Eq. 3 are greatly facilitated by the transformation to the new variable $u = m_e v^2/2e$, the electron energy in eV; we then define a new normalization for the distribution function $f(u)$ such that $\int u^{1/2} f(u) du = 1$. Figure 3 shows the results of solving Eq. 3 for $f(u)$, where the effect of an increasing electric field on the electron distribution is dramatic and produces significant high-energy tails for fields between 8 and 25 kV/m compared with the lower field cases. It is important to note that solutions to Eq. 3 do not represent an actual large-scale discharge process (*i.e*., martian lightning); instead, we have estimated the energization of a thermal core of electrons in the presence of a charging field E that interacts with the ambient CO_2 atmosphere prior to a catastrophic release of electron current in a full breakdown scenario. By far the most important implication of Eq. 3 is that the solutions are remarkably non-Maxwellian. In most cases, a Maxwellian distribution will not be a good approximation to the electron distribution for the range of electric field values we consider here (Nighan, 1970). The distribution $f(u)$ is in fact heavily modified by its interaction with CO_2 and thus must be explicitly calculated based on the relevant physical parameters for Mars, which are primarily governed by E/N, the ratio of the electric field to the neutral density.

PRODUCTION OF NEGATIVE IONS AND NEUTRALS

Once produced, the enhanced populations of electrons at higher energies will then have a markedly increased probability of impacts with other trace atmospheric constituents through a variety of interaction cross sections. While ionization processes are important, many additional reactions will occur at energies less than the ionization potentials of ambient molecules, particularly in the 4–12 eV range where dissociative attachment processes come into play. Motivated by the expected correlation between the presence of H_2O and H_2O_2 (Encrenaz *et al*., 2002), we now direct our attention to the impact of the electron distribution $f(u)$ on H_2O. For the enhanced electron population we see in $f(u)$ above 4 eV, the breakdown of H_2O via dissociative electron attachment will be a significant possibility. These reactions are outlined in Table 2. In this process, three negative ion species are possible: H^-, OH^-, and O^-. The cross section for the production of H^- is greater than those of the other negative ions by one or more orders of magnitude (Itikawa and Mason, 2005) and will be the dominant product considered here. The production rate of a prod-

TABLE 1. CO_2–ELECTRON INTERACTIONS

Process	*Mode*	*Cross sections and energy range*
CO_2–electron collisions	Momentum transfer	~4–180 × 10^{-16} cm^2 below 1 eV
CO_2 vibrational excitation	Symmetric, asymmetric, and bending modes (000 → 010,000 → 020 + 100,000 → 001, 0n0 → n00)	<3 × 10^{-16} cm^2, 0.1–20 eV
CO_2–electronic excitation	Various electronic transitions ($^3\Sigma^+_u$, $^1\Sigma^+_u$, $^1\Delta_u$ . . .)	0.01–6 × 10^{-16} cm^2, 0.1–100 eV
$CO_2 \rightarrow CO_2^+$	Impact ionization	<4 × 10^{-16} cm^2, 13.7–100 eV
$CO_2 \rightarrow CO/O^-$ dissociation	Electron dissociative attachment 4.28 × 10^{-19} cm^2 at 8.1 eV	1.5 × 10^{-19} cm^2 at 4.3 eV

After Itikawa (2002).

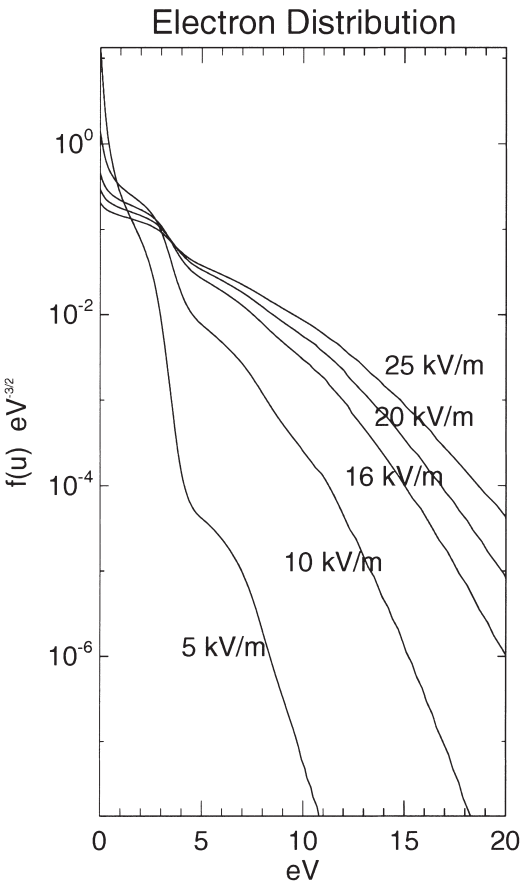

FIG. 3. The electron density distribution in the atmosphere at the surface of Mars for varying values of a dust storm-generated electric field. A neutral density of $n \sim 2 \times 10^{23}/\mathrm{m}^3$ and an initial core electron density of $n_o \sim 5 \times 10^6/\mathrm{m}^3$ is assumed. The variable u is the electron energy in eV, and $f(u)$ defined such that $\int u^{1/2} f(u) du = 1$. For electric fields >8 kV/m, a substantial high-energy tail develops.

uct n' from the electron distribution acting on a material of number density n is given by

$$\frac{dn'}{dt} = knn_e \tag{4}$$

where k is the chemical rate constant and n_e is the electron density. The presence of energized electrons in the CO_2 atmosphere will augment the production rate of any species n' in two ways: first, *via* the interaction cross sections for specific reactions that form the rate constant k, and also through increasing the degree of ionization of the atmosphere leading to larger values of n_e. Using the electron distributions obtained numerically, we can calculate the chemical rate constant based on the interaction cross sections for dissociative attachment interactions:

$$k = \langle \sigma v \rangle = \left(\frac{2e}{m_e} \right)^{1/2} \int \sigma(u) u f(u) du \tag{5}$$

where $f(u)$ is the electron distribution function we have determined using Eq. 3, u is the electron energy in eV, and $\sigma(u)$ is the energy-dependent cross section for electron–H_2O dissociative attachment.

The calculation of n_e, the bulk electron density in the presence of an electric field, follows the Townsend formalism (Llewellyn-Jones, 1981), in which n_e is given by

$$n_e = n_o e^{\alpha x} \tag{6}$$

where n_o is the initial seed electron density (due to steady-state conditions at the surface of Mars outside the influence of electric fields), α is the Townsend first ionization coefficient, and x is a physical length scale over which the electric fields persist. The Townsend coefficient α is determined similarly as with the rate constant k

$$\alpha = \frac{n_{CO_2}}{v_d} \left(\frac{2e}{m_e} \right)^{1/2} \int_{13.8\ \mathrm{eV}}^{\infty} \sigma_i(u) u f(u) du \tag{7}$$

where n_{CO_2} is the density of CO_2, $\sigma_i(u)$ is the ionization cross section for CO_2 above ~13.8 eV, and v_d is the electron drift velocity:

$$v_d = -\frac{E}{3N} \left(\frac{2e}{m_e} \right)^{\frac{1}{2}} \int_u u \frac{\partial f}{\partial u} \frac{1}{\sigma(u)} du \tag{8}$$

The constant α then describes the growth of electrons via electron–CO_2 ionization as suggested by Eq. 6. The choice of x in Eq. 6 is usually given by the electrode spacings in laboratory experiments designed to study ionization processes. In our case, we consider x to be the length scale of coherent electric fields occurring in dust events. Though x may be considerably larger, we made a conservative estimate of $x < 1$ m, based on mea-

TABLE 2. H_2O DISSOCIATIVE ATTACHMENT PROCESSES

Dissociation product	*Energy (eV)*
$O(^3P) + H_2(X)$	5.03
$OH(X) + H(n = 1)$	5.10
$O^*(^1D) + H_2(X)$	7.00
$OH^*(A) + H(n = 1)$	9.15
$O^*(^1S) + H_2(X)$	9.22
$O(^3P) + 2H$	9.51
$O^*(3s^3S^O) + H_2(X)$	14.56
$OH(X) + H^*(n = 2)$	15.30
$OH(X) + H^*(n = 3)$	17.19

Compiled by Itikawa and Mason (2005).

surements taken in terrestrial dust devils (Delory *et al.*, 2002; Farrell *et al.*, 2003) and consistent with the desire to keep $n_e << n_{CO_2}$ such that the energetic electrons remain a perturbation against the neutral background, with a degree of ionization $<10^{-5}$.

The cross sections for dissociative attachment of H_2O were compiled by Itikawa and Mason (2005) and based on measurements conducted by Melton (1972) and Compton and Christophorou (1967). The highest cross sections for negative ion production from dissociative electron attachment of H_2O are for H^-, peaking at $\sim 6.37 \times 10^{-18}$ cm^2 near ~6.4 eV, and also $\sim 1.16 \times 10^{-18}$ cm^2 near ~8.2 eV, while cross sections for OH^- and O^- production peak at values $\sim 1 \times 10^{-19}$ and $\sim 5.8 \times 10^{-19}$ cm^2, respectively. Using these cross sections and an H_2O column density of ~20 pr-μm (where pr-μm represents "precipitable micron," and 1 pr-μm $= 10^{-4}$ g/cm^2 of $H_2O = 3.35 \times 10^{18}$/cm^2 of H_2O molecules, corresponding to ~0.03% of the neutral number density at the surface), we calculate the production rates of these products as a function of electric field in Table 3. Results of similar calculations for dissociation of CO_2 into CO and O^- are also listed in Table 3. Figure 4 shows the corresponding parameters for the electron energetics and CO_2 ionization, where n_e, ν_d, α, and the rates of CO/O^- and OH/H^- production are plotted as a function of electric field E in kV/m.

DISCUSSION AND SIGNIFICANCE

Using a rigorous plasma physics approach, we arrive at a physical model, as discussed below, that reveals the impact of dust devil- and storm-generated electric fields on the atmospheric chemistry of Mars.

During virtually any dust activity arising from the ubiquitous saltation processes in dust devils or the larger dust storms, significant triboelectric charging of dust grains occurs. Subsequent lofting followed by vertical stratification of these charge carriers results in large-scale electric fields. Acting under the influence of the electric field, a population of preexisting ambient electrons becomes energized and impacts atmospheric CO_2 via a multitude of elastic, vibrational, electronic excitational, ionization, and dissociative attachment processes. The electron density n_e grows substantially as ionization of the CO_2 atmosphere occurs. The mediation between energy gained through the electric field versus the energy lost due to CO_2 interactions is expressed by the final solution to the electron distribution function $f(u)$ in Fig. 3. These distributions are remarkably non-Maxwellian, with increasing high-energy tails becoming prominent with increasing electric field. Once derived, the electron distribution $f(u)$ enables the calculation of the production rates of other chemical species. In this case, because of the importance of H_2O in the formation of H_2O_2, we examine the impact of $f(u)$ on the stability of atmospheric H_2O and find that dissociative attachment from the energized electrons leads primarily to the production of OH/H^-, followed by O^- (and either 2H or H_2) and OH/H^-.

It is important to make the distinction between a full discharge process and the electron energization that we model here. In particular, we note that the electron density expression in Eq. 6 also possesses a denominator of the form $1 - (\omega/\alpha)(e^{\alpha x} - 1)$ (Uman, 1969; Llewellyn-Jones, 1981), which is ignored in our current calculation. The variable ω is the growth rate of secondary electrons produced by the gas (electrons produced by processes other than electron/molecule impact ionization), with ω/α often referred to as Townsend's second coefficient, and x is the electrode/anode distance. If a substantial number of secondary electrons are produced in the plasma, this denominator can go to zero, thereby making

TABLE 3. CO_2 AND H_2O DISSOCIATION RATES

	Rate ($m^{-3}s^{-1}$)			
Electric field (kV/m)	$CO_2 \rightarrow CO/O^-$	$H_2O \rightarrow OH/H^-$	$H_2O \rightarrow O^-$	$H_2O \rightarrow OH^-/H$
5	4.17×10^9	1.31×10^7	5.30×10^5	2.77×10^5
10	7.75×10^{11}	3.17×10^9	1.83×10^8	7.63×10^7
16	7.53×10^{12}	3.27×10^{10}	2.85×10^9	9.30×10^8
20	1.45×10^{14}	6.24×10^{11}	6.54×10^{10}	1.93×10^{10}
25	3.38×10^{17}	1.42×10^{15}	1.75×10^{14}	4.75×10^{13}

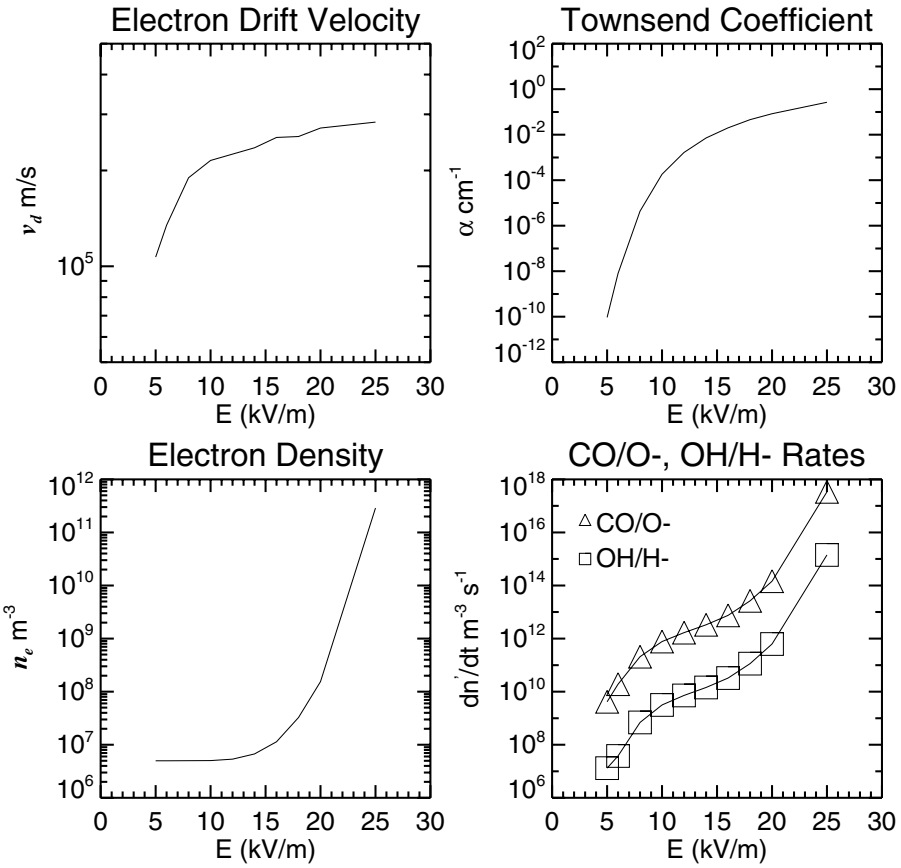

FIG. 4. The electron drift velocity (ν_d), Townsend first ionization coefficient (α), electron density (n_e), and CO_2 and H_2O dissociation rates (dn'/dt) as a function of dust storm-driven electric fields.

the electron density tend toward infinity (all bound electrons are free). This situation of complete gas breakdown defines a "filamentary" discharge like the one that occurs in terrestrial cloud-to-ground lightning. Secondary electron generation processes are difficult to quantify, and their behavior is usually a strong function of the boundary conditions imposed on the plasma. While filamentary discharge and complete gas breakdown is possible in a low-density CO_2 gas with secondaries (Llewellyn-Jones, 1981), we choose to ignore secondary processes and discharges for our martian dust storm model given the high degree of uncertainty that would then affect the reliability of the derived chemical rates for OH/H^- and other negative ion production.

Hence, by not including secondary electron generation processes ($\omega = 0$), we rule out chemistry from filamentary, ionized discharges. However, our calculations show that in pre-breakdown conditions, significant chemical reaction rates are generated even in the case where the plasma electron density is relatively small compared with the ambient density and the electron drift velocities ν_d are $<10^6$ m/s. These drift velocities describe a slow-moving, mildly ionized plasma that is very different from a typical discharge event, such as those that occur in terrestrial cloud-to-ground lightning stroke where ionization is nearly 100% and the electron speed is 0.1–0.3c (Uman, 1969). The plasma in the martian dust storms may be more reminiscent of that in terrestrial sprites: transient mesosphere luminous emissions (Rowland, 1998; Sentman *et al.*, 1995; Sentman and Wescott, 1995) that are also mildly ionized (a few percent) and relatively slow moving (Pasko *et al.*, 1995, 1997). Further, the 30–50-km region of the terrestrial atmosphere has similar pressures as the lower martian atmosphere, which suggests similar atmospheric environments for the two plasmas. Sprites result when lightning-related post-discharge electrostatic fields between the cloudtops and ionosphere become large, and create electric field-driven elec-

tron energization that acts to initiate excitation of mesospheric gas. In the martian dust devil/storm case, we are considering electrostatic fields that form between the analogous ground and dust storm top that also give rise to electric field-driven electron energization. Certainly for the case of filamentary discharges and large electron densities, Eqs. 4 and 5 indicate greater production of CO, OH, and the negative ions. However, substantial reaction rates still occur in the low-density, slow-moving corona-like plasma we have modeled here (see Fig. 4).

The rates calculated for the production of OH/H^- are particularly significant in terms of the subsequent generation of H_2O_2 (Atreya *et al*., 2006). OH/H^- production from photochemical processes alone is estimated to be $\sim 10^{10}\ m^{-3}\ s^{-1}$, while our calculations indicate that electric field-driven OH/H^- rates become equal to photochemical rates in the presence of ~10 kV/m fields and grow exponentially to orders of magnitude greater values by 20–25 kV/m. As shown by Atreya *et al*. (2006), the rates of OH/H^- production listed in Table 3 will enable the creation of H_2O_2 at rates of up to ~200 times typical photochemical rates. While the impact of electrified dust on oxidant production is potentially substantial, this process may also be limited by several key factors. First and foremost, the production of OH/H^- is clearly dependent on the amount of water vapor present, which could be the limiting factor for the subsequent generation of H_2O_2. Thus, we expect a wide variability in the efficiency of our electrochemical model, depending on the distribution and amount of H_2O available during dust events. The spatial extent and degree of electrification within martian dust storms and devils will also ultimately define limits. While discharges are common in terrestrial storm systems, macroscopic electric fields rarely exceed 400 kV/m (Winn *et al*., 1974), a fraction of the atmospheric breakdown potential of ~3,000 kV/m. This discrepancy represents an unresolved issue in terrestrial thunderstorm electrification and may indicate that breakdown potentials are highly spatially localized within a given storm and difficult to measure *in situ*. Thus, if the electrification of martian dust storms is analogous to terrestrial thunderstorms, these events may only reach some fraction of the martian breakdown potential over most of the storm volume. However, details of the charging process are likely different for dust storms on Mars compared with analogous terrestrial processes. While large-scale, macroscopic electric fields may be limited on Mars as in the terrestrial case, numerous models do admit the possibility for higher fields that approach breakdown levels on large scales (Melnik and Parrot, 1998; Farrell *et al*., 2003). Pending a verification of these electric fields using measurements from a future instrument on Mars, we include the full range of likely potentials that may be encountered within a martian dust storm such that all likely production rates can be considered.

Despite these potential limitations, there is reason to believe that dust storm-driven electrochemistry on Mars could be a compelling explanation for the degree of chemical reactivity and resulting sterility of martian soil as implied by the Viking lander results. Even if larger-scale fields are limited on Mars, reaction rates on the order of photochemical contributions will still occur for fields of ~10 kV/m, less than half of the theoretical breakdown. We have also modeled predischarge conditions only; subsequent electrical breakdown and the possibility of runaway electrons in analogy with terrestrial sprites may introduce new and more energetic electrochemical processes, albeit over short temporal and spatial scales. Additional aspects of our model relevant to enhanced oxidant production include the fact that these processes occur close to the surface, which results in a higher probability for any H_2O_2 condensate to enter the regolith before significant re-vaporization. The near-surface location of electric field-driven ion production also translates into the availability of a larger amount of ambient H_2O compared with what is available for photochemical processes at higher altitudes, which results in enhanced production of H_2O_2.

CONCLUSION

Theory and experiment provide ample evidence that dynamic dust events are nearly always significantly electrified. Using a collisional plasma physics model, we have shown that electrons acting under the influence of these electric fields in the martian atmosphere can significantly enhance the creation of chemical products that are important precursors to the production of the oxidant H_2O_2. Measurements of electric fields on Mars, obtained simultaneously with the characterization of any trace species production using a gas analyzer, would provide some observational

constraints on the importance of the electrochemical process we have outlined. Assuming that electrochemical processes in martian dust storms remain a possibility, future work will include an examination of the direct impact of energized electrons on other trace atmospheric constituents on Mars, such as methane and any organic compounds. Additionally, there is the question of the global and historical impact of atmospheric electricity on atmospheric chemistry, which depends on the spatial and temporal coverage of these events as well as their degree of large-scale electrification.

ACKNOWLEDGMENTS

Partial support for this research includes funding from NASA grant NAG5-9523, the Mars Fundamental Research Program, and the Phoenix Mars Scout Mission.

REFERENCES

Anderson, R. (1965) Electricity in volcanic clouds. *Science* 48, 1179–1189.

Atreya, S.K. and Gu, Z.G. (1994) Stability of the Martian atmosphere: is heterogeneous catalysis essential? *J. Geophys. Res*. 99, 13133–13145.

Atreya, S.K., Wong, A.-S., Renno, N.O., Farrell, W.M., Delory, G.T., Sentman, D.D., Cummer, S.A., Marshall, J., Rafkin, S.C.R., and Catling, D. (2006) Oxidant enhancement in martian dust devils and storms: implications for life and habitability. *Astrobiology* 6, 439–450.

Ballou, E., Wood, P.C., Wydeven, T., Lehwalt, M.E., and Mack, R.E. (1978) Chemical interpretation of Viking Lander 1 life detection experiment. *Nature* 271, 644–645.

Cantor, B.A., James, P.B., Caplinger, M., and Wolff, M.J. (2001) Martian dust storms: 1999 Mars Orbiter Camera observations. *J. Geophys. Res*. 106, 23653–23687.

Clancy, R.T. and Nair, H. (1996) Annual (perihelion-aphelion) cycles in the photochemical behavior of the global Mars atmosphere. *J. Geophys. Res*. 101, 12785–12790.

Compton, R.N. and Christophorou, L.G. (1967) Negative-ion formation in H_2O and D_2O. *Phys. Rev*. 154, 110–116.

Crozier, W.D. (1964) The electric field of a New Mexico dust devil. *J. Geophys. Res.* 69, 5427–5429.

Crozier, W.D. (1970) Dust devil properties. *J. Geophys. Res*. 75, 4583–4585.

Delory, G.T., Farrell, W.M., Hillard, B., Renno, N.O., Smith, P., Marshall, J.R., and Eatchel, A. (2002) The electrical structure of terrestrial dust devils: implications of multiple vertical measurements of the electric field [abstract 0335]. In *AGU Fall Meeting Abstracts, Vol. 51*, American Geophysical Union, Washington, DC.

Encrenaz, T., Greathouse, T.K., Bezard, B., Atreya, S.K., Wong, A.S., Richter, M.J., and Lacy, J.H. (2002) A stringent upper limit of the H_2O_2 abundance in the Martian atmosphere. *Astron. Astrophys*. 396, 1037–1044.

Encrenaz, T., Bezard, B., Greathouse, T.K., Richter, M.J., Lacy, J.H., Atreya, S.K., Wong, A.S., Lebonnois, S., Lefevre, F., and Forget, F. (2004) Hydrogen peroxide on Mars: evidence for spatial and seasonal variations. *Icarus* 170, 424–429.

Ette, A.I.I. (1971) The effect of the harmattan dust on atmospheric electric parameters. *J. Atmospheric Terrestrial Phys*. 33, 295–300.

Farrell, W.M., Delory, G.T., Cummer, S.A., and Marshall, J.R. (2003) A simple electrodynamic model of a dust devil. *Geophys. Res. Lett*. 30, 2050–2053.

Farrell, W.M., Smith, P.H., Delory, G.T., Hillard, G.B., Marshall, J.R., Catling, D., Hecht, M., Tratt, D.M., Renno, N., Desch, M.D., Cummer, S.A., Houser, J.G., and Johnson, B. (2004) Electric and magnetic signatures of dust devils from the 2000–2001 MATADOR desert tests. *J. Geophys. Res*. 109, E03004.

Ferri, F., Smith, P.H., Lemmon, M., and Renno, N.O. (2003) Dust devils as observed by Mars Pathfinder. *J. Geophys. Res*. 108, doi:10.1029/2000JE001421.

Fisher, J.A., Richardson, M.I., Newman, C.E., Szwast, M.A., Graf, C., Basu, S., Ewald, S.P., Toigo, A.D., and Wilson, R.J. (2005) A survey of Martian dust devil activity using Mars Global Surveyor Mars Orbiter Camera images. *J. Geophys. Res*. 110, E03004, doi:10.1029/2003JE002165.

Formisano, V., Atreya, S., Encrenaz, T., Ignatiev, N., and Giuranna, M. (2004) Detection of methane in the atmosphere of Mars. *Science* 306, 1758–1761.

Freier, G.D. (1960) The electric field of a large dust devil. *J. Geophys. Res*. 65, 3504.

Itikawa, Y. (2002) Cross sections for electron collisions with carbon dioxide. *J. Phys. Chem. Ref. Data* 31, 749–767.

Itikawa, Y. and Mason, N. (2005) Cross sections for electron collisions with water molecules. *J. Phys. Chem. Ref. Data* 34, 1–22.

Klein, H.P. (1998) The search for life on Mars: what we learned from Viking. *J. Geophys. Res*. 103, 28463–28466.

Krasnopolsky, V.A. (1993) Photochemistry of the Martian atmosphere (mean conditions). *Icarus* 101, 313–332.

Krasnopolsky, V.A. (1995) Uniqueness of a solution of a steady state photochemical problem: applications to Mars. *J. Geophys. Res*. 100, 3263–3276.

Krasnopolsky, V.A., Maillard, J.P., and Owen, T.C. (2004) Detection of methane in the martian atmosphere: evidence for life? *Icarus* 172, 537–547.

Llewellyn-Jones, F. (1981) The development of theories of the electrical breakdown of gases. In *Electrical Breakdown and Discharges in Gases. Part A: Fundamental Processes and Breakdown*, edited by E.E. Kunhardt and L.H. Luessen, Plenum Press, New York, pp. 1–71.

Mancinelli, R.L. (1989) Peroxides and the survivability of microorganisms on the surface of Mars. *Adv. Space Res*. 9, 191–195.

Martin, L.J., and Zurek, R.W. (1993) An analysis of the history of dust activity on Mars. *J. Geophys. Res*. 98, 3221–3246.

Melnik, O. and Parrot, M. (1998) Electrostatic discharge in Martian dust storms. *J. Geophys. Res*. 103, 29107–29118.

Melton, C.E. (1972) Cross sections and interpretation of dissociative attachment reactions producing OH^-, O/sup$^-$, and H^- in H_2O. *J. Chem. Phys*. 57, 4218–4225.

Mills, A.A. (1977) Dust clouds and frictional generation of glow discharges on Mars. *Nature* 268, 614.

Mumma, M.J., Novak, R.E., DiSanti, M.A., Bonev, B.P., and Dello Russo, N. (2004) Detection and mapping of methane and water on Mars [abstract 26.02]. In *DPS Meeting 36*, American Astronomical Society, Washington, DC.

Nair, H., Allen, M., Anbar, A.D., Yung, Y.L., and Clancy, R.T. (1994) A photochemical model of the Martian atmosphere. *Icarus* 111, 124–150.

Newman, C.E., Lewis, S.R., Read, P.L., and Forget, F. (2002) Modeling the Martian dust cycle. 1. Representations of dust transport processes. *J. Geophys. Res*. 107, 5123, doi:10.1029/2002JE001910.

Nighan, W.L. (1970) Electron energy distributions and collision rates in electrically excited N_2, CO, and CO_2. *Phys. Rev. A* 2, 1989–2000.

Oyama, V.I. and Berdahl, B.J. (1979) A model of Martian surface chemistry. *J. Mol. Evol*. 14, 199–210.

Oyama, V.I., Berdahl, B.J., and Carle, G.C. (1977) Preliminary findings of the Viking gas exchange experiment and a model for Martian surface chemistry. *Nature* 265, 110–114.

Pasko, V.P., Inan, U.S., Taranenko, Y.N., and Bell, T.F. (1995) Heating, ionization and upward discharges in the mesosphere due to intense quasi-electrostatic thundercloud fields. *Geophys. Res. Lett*. 22, 365–368.

Pasko, V.P., Inan, U.S., Bell, T.F., and Taranenko, Y.N. (1997) Sprites produced by quasi-electrostatic heating and ionization in the lower ionosphere. *J. Geophys. Res*. 102, 4529–4561.

Pitchford, L.C., O'Neil, S.V., and Rumble, J.R., Jr. (1981) Extended Boltzmann analysis of electron swarm experiments. *Phys. Rev. A* 23, 294–304.

Renno, N.O., Wong, A.-S., Atreya, S.K., de Pater, I., and Roos-Serote, M. (2003) Electrical discharges and broadband radio emission by Martian dust devils and dust storms. *Geophys. Res. Lett*. 30(22), 2140, doi:10.1029/2003GL017879.

Renno, N.O., Abreu, V.J., Koch, J., Smith, P.H., Hartogensis, O.K., De Bruin, H.A.R., Burose, D., Delory, G.T., Farrell, W.M., Watts, C.J., Garatuza, J., Parker, M., and Carswell, A. (2004) MATADOR 2002: a pilot field experiment on convective plumes and dust devils. *J. Geophys. Res*. 109, doi:10.1029/2003JE002219.

Rowland, H.L. (1998) Theories and simulations of elves, sprites and blue jets. *J. Atmospheric Solar-Terrestrial Phys*. 60, 831–844.

Ryan, J.A. and Lucich, R.D. (1983) Possible dust devils—vortices on Mars. *J. Geophys. Res*. 88, 11005–11011.

Schmidt, D.S., Schmidt, R.A., and Dent, J.D. (1998) Electrostatic force on saltating sand. *J. Geophys. Res*. 103, 8997–9001.

Sentman, D.D. and Wescott, E.M. (1995) Red sprites and blue jets: thunderstorm-excited optical emissions in the stratosphere, mesosphere, and ionosphere. *Phys. Plasmas* 2, 2514–2522.

Sentman, D.D., Wescott, E.M., Osborne, D.L., Hampton, D.L., and Heavner, M.J. (1995) Preliminary results from the Sprites94 aircraft campaign. 1. Red sprites. *Geophys. Res. Lett*. 22, 1205–1208.

Smith, P.H. and Lemmon, M. (1999) Opacity of the Martian atmosphere measured by the Imager for Mars Pathfinder. *J. Geophys. Res*. 104, 8975–8986.

Thomas, P. and Gierasch, P.J. (1985) Dust devils on Mars. *Science* 230, 175–177.

Uman, M.A. (1969) *Lightning*, McGraw-Hill Book Co., New York.

Viggiano, A.A. and Arnold, F. (1995) Ion chemistry and composition of the atmosphere. In *Handbook of Atmospheric Electrodynamics*, edited by H. Volland, CRC Press, Boca Raton, FL, pp. 1–26.

Whitten, R.C., Poppoff, I.G., and Sims, J.S. (1971) The ionosphere of Mars below 80 km altitude—I. Quiescent conditions. *Planet. Space Sci*. 19, 243–250.

Winn, W.P., Schwede, G.W., and Moore, C.B. (1974) Measurements of electric fields in thunderclouds. *J. Geophys. Res*. 79, 1761–1767.

Zent, A.P. and McKay, C.P. (1994) The chemical reactivity of the martian soil and implications for future missions. *Icarus* 108, 146–147.

Address reprint requests to:
Gregory T. Delory
Space Sciences Laboratory, MS 7450
University of California, Berkeley
Berkeley, CA 94720

E-mail: gdelory@ssl.berkeley.edu